Bioorganic & Medicinal Chemistry Letters 21 (2011) 299–302

Contents lists available at ScienceDirect

Bioorganic & Medicinal Chemistry Letters

journal homepage: www.elsevier.com/locate/bmcl

Receptor activity and conformational analysis of 5′-halogenated resiniferatoxin analogs as TRPV1 ligands

Kwang Su Lim [a], Dong Wook Kang [a], Yong Soo Kim [a], Myeong Seop Kim [a], Seul-Gi Park [b], Sun Choi [b], Larry V. Pearce [c], Peter M. Blumberg [c], Jeewoo Lee [a,*]

[a] Research Institute of Pharmaceutical Sciences, College of Pharmacy, Seoul National University, Seoul 151-742, Republic of Korea
[b] College of Pharmacy, Division of Life & Pharmaceutical Sciences, and National Core Research Center for Cell Signaling & Drug Discovery Research, Ewha Womans University, Seoul 120-750, Republic of Korea
[c] Laboratory of Cancer Biology and Genetics, Center for Cancer Research, National Cancer Institute, NIH, Bethesda, MD 20892, USA

ARTICLE INFO

Article history:
Received 7 October 2010
Accepted 1 November 2010
Available online 5 November 2010

Keywords:
TRPV1 agonist
TRPV1 antagonist
Partial agonist
Halogenation
Resiniferatoxin
Molecular modeling

ABSTRACT

A series of 5′-halogenated resiniferatoxin analogs have been investigated in order to examine the effect of halogenation in the A-region on their binding and the functional pattern of agonism/antagonism for rat TRPV1 heterologously expressed in Chinese hamster ovary cells. Halogenation at the 5-position in the A-region of RTX and of 4-amino RTX shifted the agonism of parent compounds toward antagonism. The extent of antagonism was greater as the size of the halogen increased (I > Br > Cl > F) while the binding affinities were similar, as previously observed for our potent agonists. In this series, 5-bromo-4-amino RTX (**39**) showed very potent antagonism with K_i (ant) = 2.81 nM, which was thus 4.5-fold more potent than 5′-iodo RTX, previously reported as a potent TRPV1 antagonist. Molecular modeling analyses with selected agonists and the corresponding halogenated antagonists revealed a striking conformational difference. The 3-methoxy of the A-region in the agonists remained free to interact with the receptor whereas in the case of the antagonists, the compounds assumed a bent conformation, permitting the 3-methoxy to instead form an internal hydrogen bond with the C4-hydroxyl of the diterpene.

Resiniferatoxin (RTX, **1**),[1,2] isolated from *Euphorbia resinifera*, is an extremely potent irritant tricyclic diterpene which structurally falls within the daphnane subclass of phorbol-related diterpenes but is set apart by its homovanillyl ester group at C-20.[3,4] RTX has proven to function pharmacologically as an ultrapotent agonist for the transient receptor potential vanilloid 1 (TRPV1) channel, displaying 10^3- to 10^4-fold greater potency than the prototypic agonist capsaicin.[5]

RTX was found to evoke large inward currents in dorsal root ganglion (DRG) neurons and TRPV1 transfected cell lines.[6] The actions of RTX are mediated by binding, with picomolar affinity, directly to the capsaicin-binding site on the TRPV1 receptor.[7] Whereas capsaicin under normal conditions produces only short term desensitization of TRPV1 mediated responses, the apparent desensitization to RTX can be of very long duration, lasting for weeks.[8,9] RTX is being developed as a potent desensitizing agent for neurons in the treatment of urinary urge incontinence and the pain associated with diabetic neuropathy, as well as for cancer pain.[10,11]

Structure–activity relationships for RTX derivatives have been investigated mostly through partial modifications starting from RTX or ROPA (resiniferonol orthophenylacetate) based on the three structural regions including the A-region (4-hydroxy-3-methoxyphenyl), B-region (C_{20} ester), and C-region (diterpene).[12–21] In the SAR of RTX, it should be noted that a divergence in potencies between ligand binding and agonism for TRPV1 ligands is frequently observed[15] and may reflect the distinction between the properties of the small fraction of the receptor at the cell surface and the predominant proportion in internal membranes.[22]

Previous SAR indicated that although most modifications of RTX reduced binding affinity and agonism, several have proven to be of considerable interest (Fig. 1). 5-Iodination in the A-region of RTX shifted the activity from agonism to antagonism providing a potent antagonist, 5-iodo RTX (**2**), for both rat and human TRPV1.[16,17] Surprisingly, the carbonate surrogate (**3**) in the B-region of 5-iodo RTX showed excellent agonism rather than antagonism and its

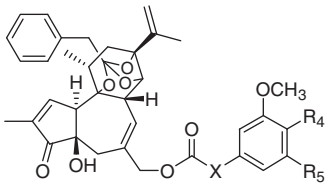

	X	R_4	R_5
1	CH_2	OH	H
2	CH_2	OH	I
3	O	OH	I
4	CH_2	$NHSO_2CH_3$	H

Figure 1.

* Corresponding author. Tel.: +82 2 880 7846; fax: +82 2 888 0649.
E-mail address: jeewoo@snu.ac.kr (J. Lee).

0960-894X/$ - see front matter © 2010 Elsevier Ltd. All rights reserved.
doi:10.1016/j.bmcl.2010.11.012

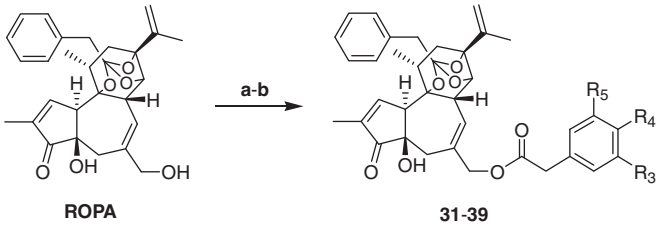

Scheme 1. Reagents and conditions: (a) R-CO_2H, EDC, CH_2Cl_2, 70–90%; (b) CF_3CO_2H/CH_2Cl_2 (1:2) for MOM deprotection, 60–96%.

potency was 4-fold higher than RTX with a one-digit picomolar value reported for hTRPV1 expressed in HEK cells.[21] Substitution of an isosteric methanesulfonamide on RTX provided a metabolically stable and potent agonist (**4**), which was 2.5-fold more potent than RTX with an EC_{50} = 0.106 nM for rat TRPV1 heterologously expressed in CHO cells.[20] The results demonstrated that halogenation and isosteric substitution of the phenolic group in the A-region appear to be key modifications influencing the functional activity and potency toward TRPV1.

In this Letter, we have investigated the effect of halogenation in the A-region of RTX and of the isosteric 4-amino surrogate in a systematic manner and we describe the synthesis and receptor activity, as well as conformational analysis for explaining the observed functional differences.

The halogenated RTX analogs (**31**–**39**) were prepared starting from commercially available ROPA (resiniferonol-9,13,14-orthophenylacetate) by the condensation with the corresponding 2-phenyl acetic acids (A-region) using EDC (1-[3-(dimethylamino)propyl]-3-ethylcarbodiimide hydrochloride) coupling reagent, followed by appropriate O-deprotection if needed (Scheme 1).

The syntheses of the A-region are represented in Schemes 2–6. The 5-fluoro-4-hydroxyphenyl A-region was prepared from 2-fluoro-6-methoxyphenol employing regioselective formylation (Scheme 2) and the 5-chloro and 5-bromo-4-hydroxyphenyl A-regions were synthesized starting from vanillin and homovanillic acid using electrophilic addition of halogens, respectively (Schemes 2 and 3). The 3,5-dibromophenyl A-region was synthesized from 1,3-dibromo-5-fluorobenzene by nucleophilic substitution of ethyl cyanoacetate followed by decarboxylation (Scheme 4). The 5-fluoro-4-amino A-region was prepared from 1,3-difluoro-2-nitrobenzene employing the reactions of Makosza's vicarious

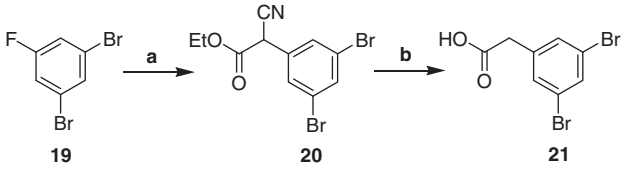

Scheme 4. Reagents and conditions: (a) ethyl cyanoacetate, NaH, DMF, 25%; (b) NaOH, H_2O 100%.

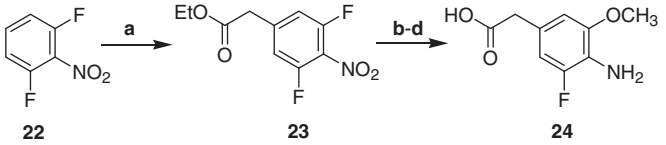

Scheme 5. Reagents and conditions: (a) *t*-BuOK, ethyl chloroformate, NMP, 22%; (b) NaOMe, MeOH, 55%; (c) Pd/C, H_2, MeOH, 69%; (d) LiOH, THF–H_2O, 82%.

nucleophilic substitution[23] and selective nucleophilic substitution of the methoxy group (Scheme 5). The 4-amino, 5-chloro and 5-bromo-4-amino A-regions were synthesized from (3-hydroxyphenyl)-acetic acid by nitration followed by halogenation of the 4-aminophenyl (Scheme 6).

The halogenated resiniferatoxin analogs were evaluated for their binding affinities (expressed as K_i values) using a competitive binding assay with [^{3}H]RTX and for their agonism/antagonism using a functional $^{45}Ca^{2+}$ uptake assay (expressed as EC_{50} and K_i (ant) values) for rat TRPV1 heterologously expressed in Chinese hamster ovary (CHO) cells.[24] In this system, resiniferatoxin displayed K_i = 0.043 nM and EC_{50} = 0.27 nM.[20] The receptor binding and functional activities of the halogenated RTX analogs are listed in Table 1.

Starting with RTX, 5-halogenation on the A-region progressively shifted the agonism toward antagonism as the size of halogen increased. 5-Fluoronation and 5-chlorination yielded the full agonists **31** and **32**, which were 9- and 21-fold less potent, respectively, than RTX for their functional activity. 5-Bromination caused a partial shift in function, providing the partial antagonist **33** with K_i (ant) = 7.2 nM and 19% residual agonism. Finally, 5-iodination (I-RTX) afforded the full antagonist **2** with K_i (ant) = 12.2 nM under the same assay conditions. The 5-halogenated RTX analogs (**31**–**33**) bound

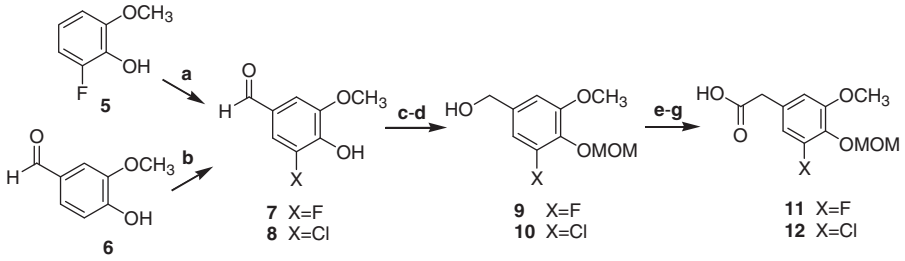

Scheme 2. Reagents and conditions: (a) (i) formaldehyde, diethylamine, EtOH, reflux, (ii) CH_3I, CH_2Cl_2, rt, 18 h, (iii) HMTA, HOAc–H_2O, 120 °C, 2 h, 37% for 3 steps; (b) NCS, NaH, THF, 49%; (c) MOMCl, DIPEA, CH_3CN, 68% for X=F, 87% for X=Cl; (d) LAH, THF, 98% for X=F and Cl; (e) CBr_4, PPh_3, benzene, 48% for X=F, 32% for X=Cl; (f) X=F: NaCN, DMF, 80 °C, 93%, X=Cl: KCN, 18-crown-6, CH_3CN, 85%; (g) NaOH, THF–H_2O, reflux, 99% for X=F and Cl.

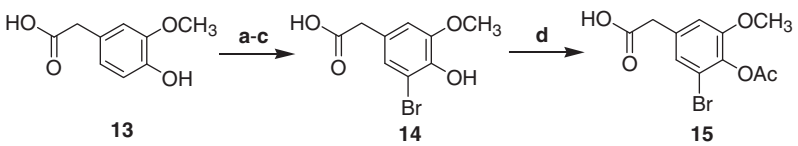

Scheme 3. Reagents and conditions: (a) cat. H_2SO_4, EtOH, 99%; (b) oxone, NaBr, acetone–H_2O, 56%; (c) NaOH, THF–H_2O, 100%; (d) Ac_2O, cat. H_2SO_4, CH_2Cl_2, 95%.

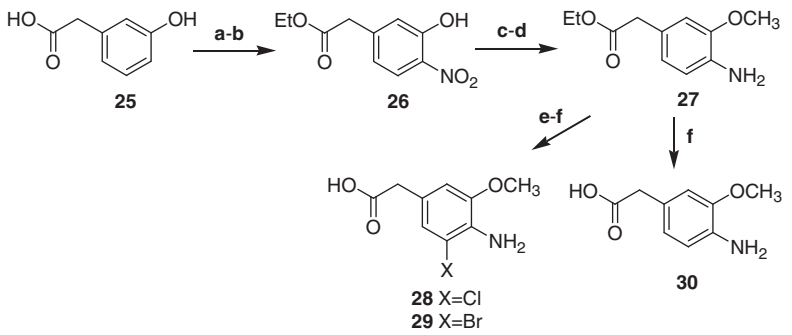

Scheme 6. Reagents and conditions: (a) cat. H_2SO_4, EtOH, 98%; (b) HNO_3, AcOH, 29%; (c) K_2CO_3, CH_3I, acetone, 71%; (d) 10% Pd/C, H_2, THF–EtOH, 97%; (e) oxone, NaCl or NaBr, acetone–H_2O, 30%; (f) LiOH, THF–H_2O, 60–90%.

Table 1
Potencies of RTX analogs for binding to rat TRPV1 and for inducing calcium influx in CHO/TRPV1 cells

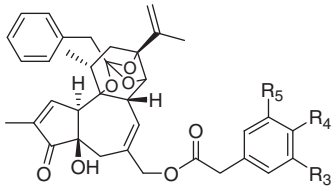

	R_3	R_4	R_5	RTX binding[a] (K_i = nM)	Ago[a,b] (EC_{50} = nM)	Ant[a,c] (K_i = nM)
1 (RTX)	OCH_3	OH	H	0.043	0.27	NE
2 (I-RTX)	OCH_3	OH	I	0.61 ± 0.08	NE	12.2 ± 4.0
31	OCH_3	OH	F	0.26 ± 0.04	1.88 ± 0.24	NE
32	OCH_3	OH	Cl	1.03 ± 0.14	5.7 ± 1.7	NE
33	OCH_3	OH	Br	0.17 ± 0.05	(19%)	7.2 ± 1.6
34	OCH_3	OAc	Br	0.30 ± 0.02	(37%)	(30%)
35	Br	H	Br	110 ± 36	1070 ± 110	NE
36	OCH_3	NH_2	H	0.13 ± 0.03	0.46 ± 0.10	NE
37	OCH_3	NH_2	F	0.70 ± 0.16	1.14 ± 0.23	NE
38	OCH_3	NH_2	Cl	0.85 ± 0.02	(34%)	(56%)
39	OCH_3	NH_2	Br	1.99 ± 0.27	NE	2.81 ± 0.26

NE, no effect.
[a] Values represent the mean ± SEM of three or more independent experiments for K_i or EC_{50}.
[b] Values in parentheses represent the mean % of agonism relative to capsaicin.
[c] Values in parentheses represent the mean % of antagonism of the capsaicin stimulated $^{45}Ca^{2+}$ uptake response.

to TRPV1 with lower affinity than did RTX (**1**) but showed little difference as the size of the halogen increased, with a range of K_i = 0.17–1.03 nM. Compound **34**, the *O*-acetyl analog of **33**, displayed modestly weaker binding affinity and antagonism compared to **33**. The 3,5-dibromo analog **35** was a full agonist, albeit with weaker binding affinity and agonist potency.

Next, the halogenated 4-amino RTX analogs were explored as bioisosteres of the corresponding 4-phenolic agonists. The parent 4-amino RTX (**36**) showed high affinity binding and potent full agonism. The values of K_i = 0.13 nM and EC_{50} = 0.46 nM were only 2–3 fold less potent than RTX. As was the case with the 5-halogenated RTX derivatives, 5-halogenation on the A-region in 4-amino RTX also shifted the agonism toward antagonism progressively as the size of the halogen increased. 5-Fluoronation produced full agonist **37**, which was 2.5-fold less potent than the parent **36**, as found in the RTX series. However, 5-chlorination already started to shift the agonism of **36** toward antagonism to afford the partial antagonist **38** and 5-bromination yielded the full antagonist **39**. Of particular note, compound **39** displayed high potency as an antagonist with K_i (ant) = 2.81 nM, which was 4-fold better than I-RTX under the same assay conditions. As found in the RTX series, the binding affinities of the 5-halogenated 4-amino RTX analogs (**37**–**39**) were weaker than that of 4-amino RTX (**36**) and little difference was examined as the size of the halogen increased, with a range of K_i = 0.7–1.99 nM. Unfortunately, the 5-iodo 4-amino analog could not be investigated due to synthetic difficulty.

In order to investigate the structural basis for the difference in the functional activities of the TRPV1 agonists and their halogenated analogs as antagonists, we performed conformational analysis of RTX (**1**) and **36** as agonists and I-RTX (**2**) and **39** as antagonists using the SYBYL Grid Search method.[25] The resulting lowest energy conformers are as shown in Figure 2 in which overlays of RTX vs I-RTX and **36** vs **39** are represented in Figure 2A and B, respectively.

In their lowest energy conformers, the antagonists **2** and **39** showed bent conformations in which the methoxy group appeared to form an intramolecular hydrogen bond with the C-4 hydroxyl group of the diterpene core. In contrast, the agonists did not show this intramolecular hydrogen-bond in their lowest conformers and instead allowed the A-region to remain free to interact with residues in the binding site. The analysis indicates that the 5-halogen promoted bending of the B-region to permit this internal hydrogen-bond formation between 3-methoxy of the A-region and C4-OH of the diterpene and the preference for this conformation was higher as the size of the halogen increased. A prediction is thus that the binding of this bent conformation, unlike the more

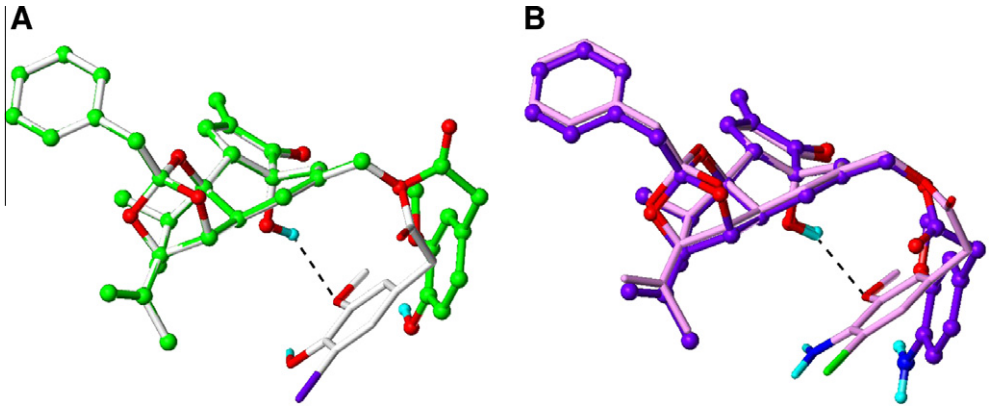

Figure 2. The lowest energy conformers of (A) RTX and I-RTX, and (B) **36** and **39**. Carbon atoms are shown in green for RTX, white for I-RTX, purple for **36** and pink for **39**. Agonists RTX and **36** are depicted as ball-and-stick. Antagonists I-RTX and **39** are depicted as capped stick. Hydrogen bonds are displayed in black dashed lines, and non-polar hydrogens are undisplayed for clarity.

extended conformation of RTX agonists, should fail to induce the shift in the conformation of the tetrameric TRPV1 channel associated with channel opening. This model thus suggests novel strategies for antagonist design.

In conclusion, we have systematically modified the aromatic A-region of RTX and its 4-amino surrogate by halogenation at the 5-position in order to explore the role of halogens in the reversal of activity from agonism to antagonism. 5-Halogenation converted the agonists to partial or full antagonists, and the extent of antagonism reflected the order of I > Br > Cl > F. Antagonism was further favored in derivatives of the 4-amino RTX surrogate compared to derivatives of RTX itself. Of particular note, the 5-bromo 4-amino RTX analog (**39**) was a potent, full antagonist with K_i (ant) = 2.81 nM, which was 4.5-fold more potent than I-RTX (**2**) under our conditions. Molecular modeling of selected agonists and antagonists demonstrated that the 3-methoxy of the A-region in agonists remained free to interact with the receptor for agonism, whereas a 5-halogen in the antagonists favored a bent B-region, allowing the 3-methoxy to form an intramolecular hydrogen bond with the C4-hydroxyl of the diterpene.

Acknowledgments

This research was supported by Grant R11-2007-107-02001-0 from the National Research Foundation of Korea (NRF), the National Core Research Center (NCRC) program (R15-2006-020) of MEST and NRF through the Center for Cell Signaling & Drug Discovery Research at Ewha Womans University (to S. Choi), and by the Intramural Research Program of the National Institutes of Health, Center for Cancer Research, National Cancer Institute. We thank numerous research fellows for some of the biological analyses.

References and notes

1. Appendino, G.; Szallasi, A. *Life Sci.* **1997**, *60*, 681.
2. Blumberg, P. M.; Szallasi, A.; Acs, G. In *Capsaicin in the study of pain*; Wood, J. N., Ed.; Academic Press: London, 1993; pp 45–62. Chapter 3.
3. Hergenhahn, M.; Adolf, W.; Hecker, E. *Tetrahedron Lett.* **1975**, *19*, 1595.
4. Adolf, W.; Sorg, B.; Hergenhahn, M.; Hecker, E. *J. Nat. Prod.* **1982**, *45*, 347.
5. Szallasi, A.; Blumberg, P. M. *Neuroscience* **1989**, *30*, 515.
6. Szallasi, A.; Szabo, T.; Biro, T.; Modarres, S.; Blumberg, P. M.; Krause, J. E.; Cortright, D. N.; Appendino, G. *Br. J. Pharmacol.* **1999**, *128*, 428.
7. Biro, T.; Acs, G.; Acs, P.; Modarres, S.; Blumberg, P. M. *J. Investig. Dermatol. Symp. Proc.* **1997**, *2*, 56.
8. Liu, L.; Simon, S. A. *Brain Res.* **1998**, *809*, 246.
9. Szallasi, A.; Joo, F.; Blumberg, P. M. *Brain Res.* **1989**, *503*, 68.
10. Bley, K. R. *Expert Opin. Investig. Drugs* **2004**, *13*, 1445.
11. Brown, D. C.; Iadarola, M. J.; Perkowski, S. Z.; Erin, H.; Shofer, F.; Laszlo, K. J.; Olah, Z.; Mannes, A. J. *Anesthesiology* **2005**, *103*, 1052.
12. Acs, G.; Lee, J.; Marquez, V. E.; Wang, S.; Milne, G. W. A.; Lewin, N. E.; Blumberg, P. M. *J. Neurochem.* **1995**, *65*, 301.
13. Walpole, C. S. J.; Bevan, S.; Bloomfield, G.; Breckenridge, R.; James, I. F.; Ritchie, T.; Szallasi, A.; Winter, J.; Wrigglesworth, R. *J. Med. Chem.* **1996**, *39*, 2939.
14. Appendino, G.; Cravotto, G.; Palmisano, G.; Annunziata, R.; Szallasi, A. *J. Med. Chem.* **1996**, *39*, 3123.
15. Acs, G.; Lee, J.; Marquez, V. E.; Blumberg, P. M. *Mol. Brain Res.* **1996**, *35*, 173.
16. Wahl, P.; Foged, C.; Tullin, S.; Thomsen, C. *Mol. Pharmacol.* **2001**, *59*, 9. Iodo-RTX.
17. Seabrook, G. R.; Sutton, K. G.; Jarolimek, W.; Hollingworth, G. J.; Teague, S.; Webb, J.; Clark, N.; Boyce, S.; Kerby, J.; Ali, Z.; Chou, M.; Middleton, R.; Kaczorowski, G.; Jones, A. B. *J. Pharmacol. Exp. Ther.* **2002**, *303*, 1052.
18. McDonnell, M. E.; Zhang, S.-P.; Dubin, A. E.; Dax, S. L. *Bioorg. Med. Chem. Lett.* **2002**, *12*, 1189.
19. Appendino, G.; Ech-Chahad, A.; Minassi, A.; Bacchiega, S.; De Petrocellis, L.; Di Marzo, V. *Bioorg. Med. Chem. Lett.* **2007**, *17*, 132.
20. Choi, H.-K.; Choi, S.; Lee, Y.; Kang, D. W.; Ryu, H.; Maeng, H.-J.; Chung, S.-J.; Pavlyukovets, V. A.; Pearce, L. V.; Toth, A.; Tran, R.; Wang, Y.; Morgan, M. A.; Blumberg, P. M.; Lee, J. *Bioorg. Med. Chem.* **2009**, *17*, 690.
21. Appendino, G.; Ech-Chahad, A.; Minassi, A.; De Petrocellis, L.; Di Marzo, V. *Bioorg. Med. Chem. Lett.* **2010**, *20*, 97.
22. Toth, A.; Blumberg, P. M.; Chen, Z.; Kozikowski, A. P. *Mol. Pharmacol.* **2004**, *65*, 282.
23. Stahly, G. P.; Stahly, B. C.; Lilje, K. C. *J. Org. Chem.* **1984**, *49*, 579.
24. Wang, Y.; Szabo, T.; Welter, J. D.; Toth, A.; Tran, R.; Lee, J.; Kang, S. U.; Lee, Y.-S.; Min, K. H.; Suh, Y.-G.; Park, M.-K.; Park, H.-G.; Park, Y.-H.; Kim, H.-D.; Oh, U.; Blumberg, P. M.; Lee, J. *Mol. Pharm.* **2002**, *62*, 947 [published erratum appears in *Mol. Pharmacol.* **2003**, *63*, 958].
25. The 3D structures of the tested compounds were generated with Concord and energy minimized using an MMFF94s force field and MMFF94 charge until the rms of the Powell gradient was 0.05 kcal mol^{-1} A^{-1} in SYBYL 8.1.1 (Tripos Int., St. Louis, MO, USA).
The conformational analysis of each compound was performed using SYBYL Grid Search method (force field: MMFF94s; charges: MMFF94; minimization method: powell; termination: gradient 0.05 kcal mol^{-1} A^{-1}; and max iterations: 10,000). The torsion angles defined for the Grid Search were C29–C14–O10–C7, C14–O10–C7–C8, O10–C7–C8–C1 and O1–C16–C33–C34 and they were altered in 30° increments. 20,736 unique conformers were produced for each compound. Among them, the lowest energy conformers were selected and the resulting conformers were superimposed using the Fit Atoms tool in SYBYL. All computational calculations were undertaken on an Intel® XeonTM Quad-core workstation with Linux Cent OS release 4.6.

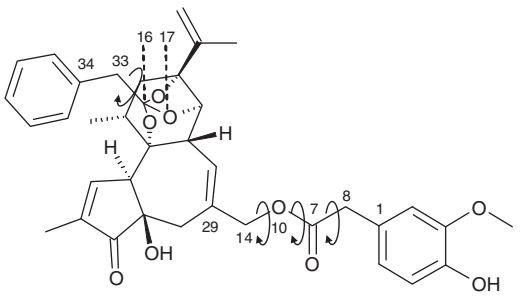

RTX